



1 **Examination of varying mixed-phase stratocumulus clouds in terms of their**
2 **properties, ice processes and aerosol-cloud interactions between polar and**
3 **midlatitude cases: An attempt to propose a microphysical factor to explain the**
4 **variation**

5

6 Seung Soo Lee^{1,2,3}, Chang-Hoon Jung⁴, Young Jun Yoon⁵, Junshik Um^{6,7}, Youtong
7 Zheng⁸, Jianping Guo⁹, Manguttathil. G. Manoj¹⁰, Sang-Keun Song¹¹

8

9 ¹Science and Technology Corporation, Hampton, Virginia

10 ²Earth System Science Interdisciplinary Center, University of Maryland, College Park,
11 Maryland, USA

12 ³Research Center for Climate Sciences, Pusan National University, Busan, Republic of
13 Korea

14 ⁴Department of Health Management, Kyungin Women's University, Incheon, Republic of
15 Korea

16 ⁵Korea Polar Research Institute, Incheon, Republic of Korea

17 ⁶Department of Atmospheric Sciences, Pusan National University, Busan, Republic of
18 Korea

19 ⁷Institute of Environmental Studies, Pusan National University, Busan, Republic of Korea

20 ⁸Department of Earth and Atmospheric Sciences, University of Houston, Houston, Texas,
21 USA

22 ⁹State Key Laboratory of Severe Weather, Chinese Academy of Meteorological Sciences,
23 Beijing 100081, China



24 ¹⁰Advanced Centre for Atmospheric Radar Research, Cochin University of Science and
25 Technology, Kerala, India

26 ¹¹Department of Earth and Marine Sciences, Jeju National University, Jeju, Republic of
27 Korea

28

29

30

31

32

33

34

35

36

37

38

39

40

41

42

43

44

45

46

47

48 Corresponding author: Seoung Soo Lee

49 Office: (303) 497-6615

50 Cell: (609) 375-6685

51 Fax: (303) 497-5318

52 E-mail: cumulss@gmail.com, slee1247@umd.edu



53 **Abstract**

54

55 This study examines the ratio of ice crystal number concentration (ICNC) to cloud droplet
56 number concentration (CDNC), which is ICNC/CDNC, as a microphysical factor that
57 induces differences in cloud development, its interactions with aerosols and impacts of ice
58 processes on them among cases of mixed-phase clouds. This examination is performed
59 using a large-eddy simulation (LES) framework and one of efforts toward a more general
60 understanding of mechanisms controlling those development and impacts in mixed-phase
61 clouds. For the examination, this study compares a case of polar mixed-phase clouds to
62 that of midlatitude mixed-phase clouds with weak precipitation. It is found that
63 ICNC/CDNC plays a critical role in making differences in cloud development with respect
64 to the relative proportion of liquid and ice mass between the cases by affecting in-cloud
65 latent-heat processes. Note that this proportion has an important implication for cloud
66 radiative properties and thus climate. It is also found that ICNC/CDNC plays a critical role
67 in making differences in clouds and their interactions with aerosols and impacts of ice
68 processes on them between the cases by affecting in-cloud latent-heat processes. Findings
69 of this study suggest that ICNC/CDNC can be a simplified general factor that contributes
70 to a more general understanding of mixed-phase clouds and roles of ice processes and
71 aerosols in them and thus, to the development of more general parameterizations of those
72 clouds and roles.

73

74

75

76

77

78

79

80

81

82

83



84 **1. Introduction**

85

86 It is well-known that stratiform clouds (e.g., stratus and stratocumulus clouds) have
87 significant impacts on climate (Warren et al. 1986; Stephens and Greenwald 1991;
88 Hartmann et al. 1992; Hahn and Warren 2007; Wood, 2012; Dione et al., 2019; Zheng et
89 al., 2021). Since industrialization, there have been increases in aerosol concentrations and
90 this has had impacts on stratiform clouds and climate (Twomey, 1974; Albrecht, 1989).
91 However, our level of understanding of these clouds and impacts has been low and this has
92 caused the highest uncertainty in the prediction of future climate (Ramaswamy et al., 2001;
93 Forster et al., 2007; Knippertz et al., 2011; Hannak et al., 2017). Stratiform clouds can be
94 classified into warm and mixed-phase clouds. Mixed-phase clouds involve ice processes
95 and frequently form in midlatitude and polar regions. Most previous studies have focused
96 on warm clouds and their interactions with aerosols, whereas the mixed-phase clouds and
97 their interactions with aerosols are poorly understood mainly due to the more complex ice
98 processes. Hence, mixed-phase clouds and their interactions with aerosols account for the
99 uncertainty more than warm clouds and their interactions with aerosols (Ramaswamy et al.,
100 2001; Forster et al., 2007; Wood, 2012; IPCC, 2021; Li et al., 2022).

101 It is known that the relative proportion of liquid mass, which can be represented by
102 liquid-water content (LWC) or liquid-water path (LWP), and ice mass, which can be
103 represented by ice-water content (IWC) or ice-water path (IWP), in mixed-phase stratiform
104 clouds plays a critical role in cloud radiative properties and thus their climate feedbacks
105 (Choi et al., 2010 and 2014). This is because radiative properties of liquid particles are
106 substantially different from those of ice particles. The relative proportion is defined to be
107 IWC (IWP) over LWC (LWP) or IWC/LWC (IWP/LWP) in this study. Motivated by this
108 and the above-mentioned uncertainty, this study aims to improve our understanding of
109 mixed-phase stratiform clouds and their interactions with aerosols with the emphasis on
110 ice processes and IWC/LWC (or IWP/LWP).

111 Lee et al. (2022) have investigated mixed-phase stratocumulus clouds in a midlatitude
112 region and found that microphysical latent-heat processes are more important in the
113 development of mixed-phase clouds and their interactions with aerosols than entrainment
114 and sedimentation processes. Lee et al. (2022) have found that a microphysical factor, the



115 ratio of ice crystal number concentration (ICNC) to cloud droplet number concentration
116 (CDNC) or ICNC/CDNC, play an important role in latent processes, the development of
117 mixed-phase clouds and their interactions with aerosols. In particular, Lee et al. (2022)
118 have found that IWC/LWC or IWP/LWP is strongly affected by ICNC/CDNC. This is
119 because deposition (condensation) of water vapor occurs on the surface of ice crystals
120 (droplets). Thus, they act as sources of deposition (condensation) and then IWC or IWP
121 (LWC or LWP). More ice crystals (droplets) provide the greater integrated surface area of
122 ice crystals (droplets) and induce more deposition (condensation) for a given
123 environmental condition (Lee et al., 2009; Khain et al., 2012; Fan et al., 2018; Chua and
124 Ming, 2020; Lee et al., 2022). Note that deposition and condensation are processes through
125 which water vapor is removed, hence ice crystals and droplets are sinks of water vapor
126 when deposition and condensation occur. However, when it comes to deposition and
127 condensation themselves as microphysical processes, ice crystals (droplets) can be
128 considered the sources of deposition and condensation. The higher ICNC/CDNC means
129 more ice crystals or sources of deposition per a droplet as a source of condensation in a
130 given group of ice crystals and droplets. Thus, the higher ICNC/CDNC enables more
131 deposition per unit condensation to occur, which can raise IWC/LWC or IWP/LWP.

132 Mixed-phase stratocumulus clouds in different regions are known to have different
133 IWC/LWC or IWP/LWP and aerosol-cloud interactions (e.g., Choi et al., 2010). Lots of
134 factors such as environmental conditions, which can be represented by variables such as
135 stability, humidity and wind shear, can explain those differences. It is important to establish
136 a general principle that explains the differences, since the general principle is useful in the
137 development of a more general or comprehensive parameterization of stratocumulus clouds
138 and their interactions with aerosols for climate models. This contributes to the better
139 prediction of future climate, considering that the absence of the comprehensive
140 parameterization has been considered one of the biggest obstacles to the better prediction
141 (Ramaswamy et al., 2001; Foster et al., 2007; Stevens and Feingold, 2009). As a way of
142 contributing to the establishment of the general principle, this study attempts to take
143 ICNC/CDNC as a general factor, which can constitute the general principle, to explain the
144 differences in IWC/LWC (or IWP/LWP) and aerosol-cloud interactions among clouds.
145 This study also attempts to elucidate how ice processes differentiate mixed-phase clouds



146 from warm clouds in terms of cloud development and its interactions with aerosols, and
147 how this differentiation varies among cases of mixed-phase clouds with different
148 ICNC/CDNC values. This attempt is valuable, considering that it is generally accepted that
149 the establishment of the general principle for stratocumulus clouds has been progressed
150 much less than that for other types of clouds such as convective clouds. The attempt is
151 valuable, also considering that our level of understanding of how ice processes differentiate
152 mixed-phase clouds and their interactions with aerosols from much-studied warm clouds
153 and their interactions with aerosols has been low.

154 For the attempt, this study investigates a case of mixed-phased stratiform clouds in
155 the polar region. Via the investigation, this study aims to identify process-level
156 mechanisms that control the development of those clouds and their interactions with
157 aerosols, and the impact of ice processes on the development and interactions using a large-
158 eddy simulation (LES) framework. Then, this study compares the mechanisms in the case
159 of polar clouds to those in a case of midlatitude clouds which have been examined by Lee
160 et al. (2022). Through this comparison, this study tests ICNC/CDNC as a general factor,
161 which contributes to the establishment of the general principle, to explain the differences
162 in IWC/LWC (or IWP/LWP) and aerosol-cloud interactions among cases of mixed-phased
163 stratiform clouds. Through this comparison, this study also identifies how ICNC/CDNC
164 contributes to different roles of ice processes in the differentiation between mixed-phase
165 and warm clouds among cases of mixed-phase stratiform clouds.

166

167 **2. Case, model and simulations**

168

169 **2.1 LES model**

170

171 LES simulations are performed by using the Advanced Research Weather Research and
172 Forecasting (ARW) model. A bin scheme, which is detailed in Khain et al. (2000) and
173 Khain et al. (2011), is adopted by the ARW for the simulation of microphysics. Size
174 distribution functions for each class of hydrometeors, which are classified into water drops,
175 ice crystals (plate, columnar and branch types), snow aggregates, graupel and hail, and
176 aerosols acting as cloud condensation nuclei (CCN) and ice-nucleating particles (INP) are



177 represented with 33 mass doubling bins, i.e., the mass of a particle m_k in the k th bin is
178 determined as $m_k = 2m_{k-1}$. Each of hydrometeors has its own terminal velocity that varies
179 with the hydrometeor mass and the sedimentation of hydrometeors is simulated using their
180 terminal velocity. The evolution of aerosol size distribution at each grid point is controlled
181 by aerosol sinks and sources such as aerosol advection, turbulent mixing and activation. It
182 is assumed that aerosols do not fall down by themselves and move around by airflow that
183 is composed of horizontal flow, updrafts, downdrafts and turbulent motions. When aerosols
184 move with airflow, it is assumed that they move with the same velocity as airflow. Taking
185 activation as an example of the evolution of aerosol size distribution, the bins of the aerosol
186 spectra that correspond to activated particles are emptied. Activated aerosol particles are
187 included in hydrometeors and move to different classes and sizes of hydrometeors through
188 collision-coalescence. In case hydrometeors with aerosol particles precipitate to the surface,
189 those particles are removed from the atmosphere.

190 The large energetic turbulent eddies are directly resolved by the LES framework, and
191 the effects of the smaller subgrid-scale turbulent motions on the resolved flow are
192 parameterized based on the most widely used method that was proposed by Smagorinsky
193 (1963) and Lilly (1967). In this method, the mixing time scale is defined to be the norm of
194 the strain rate tensor (Bartosiewicz and Duponcheel, 2018). A cloud-droplet nucleation
195 parameterization based on Köhler theory represents cloud-droplet nucleation. Arbitrary
196 aerosol mixing states and aerosol size distributions can be fed to this parameterization. To
197 represent heterogeneous ice-crystal nucleation, the parameterizations by Lohmann and
198 Diehl (2006) and Möhler et al. (2006) are used. In these parameterizations, contact,
199 immersion, condensation-freezing, and deposition nucleation paths are all considered by
200 taking into account the size distribution of INP, temperature and supersaturation.
201 Homogeneous aerosol (or haze particle) and droplet freezing is
202 also considered following the theory developed by Koop et al. (2000).

203 The bin microphysics scheme is coupled to the Rapid Radiation Transfer Model
204 (RRTM; Mlawer et al., 1997). The effective sizes of hydrometeors, which are calculated
205 in the bin scheme, are fed into the RRTM as a way of considering effects of the effective
206 sizes on radiation. The surface process and resultant surface heat fluxes are simulated by
207 the interactive Noah land surface model (Chen and Dudhia, 2001).



208

209

2.2 Case and simulations

210

211

2.2.1 Case and standard simulations

212

213 In the Svalbard area, Norway, a system of mixed-phase stratocumulus clouds was observed
214 to exist over a period between 02:00 local solar time (LST) and 20:00 LST on March 29th,
215 2017. On average, the bottom and top of these clouds are at ~400 m and ~3 km in altitude,
216 respectively. The simulation of the observed system or case, i.e., the control run, is
217 performed for the period on a three-dimensional domain of which horizontal extent is
218 marked by a red rectangle in Figure 1. A 100-m resolution is adopted by the horizontal
219 domain in the control run. The length of the domain in the horizontal directions is 50 km.
220 The length of the domain in the vertical direction is ~5 km and the resolution for the vertical
221 domain gets coarsened with height from ~20 m just above the surface to ~100 m at the
222 model top. Potential temperature, specific humidity, and wind as initial and boundary
223 conditions, which represent synoptic-scale environment, for the control run are provided
224 by reanalysis data that are produced by Met Office Unified Model (Brown et al., 2012)
225 every 6 hours on a $0.11^\circ \times 0.11^\circ$ grid. The control run employs an open lateral boundary
226 condition. Figure 2 shows the vertical distribution of the domain-averaged potential
227 temperature and humidity at the first time step. There is a neutral, mixed layer between the
228 surface and 1 km in altitude as an initial condition (Figure 2).

229

230

231

232

233

234

235

236

237

There is a ground station in the domain (Tunved et al., 2013; Jung et al., 2018). This station measures the properties of cloud condensation nuclei (CCN) such as the number concentration, size distribution and composition. The measurement by the station indicates that on average, aerosol particles are an internal mixture of 70 % ammonium sulfate and 30 % organic compound. This mixture is assumed to represent aerosol chemical composition over the whole domain and simulation period for this study. The observed and averaged concentration of aerosols acting as CCN is $\sim 200 \text{ cm}^{-3}$ over the simulation period. Based on this, 200 cm^{-3} as an averaged concentration of aerosols acting as CCN is interpolated into all of grid points immediately above the surface at the first time step.



238 Aerosol effects on radiation before aerosol is activated are not taken into account for
239 this study, since there is no significant amount of radiation absorbers in the mixture. Based
240 on observation, the size distribution of aerosols acting as CCN is assumed to be a tri-modal
241 log-normal distribution (Figure 3). The shape of distribution, which is a tri-modal log-
242 normal distribution, as shown in Figure 3 is applied to the size distribution of aerosols
243 acting as CCN in all parts of the domain during the whole simulation period. The assumed
244 shape in Figure 3 is obtained by performing the average on the size distribution parameters
245 (i.e., modal radius and standard deviation of each of nuclei, accumulation and coarse modes,
246 and the partition of aerosol number among those modes) over the simulation period. It is
247 assumed that the interpolated CCN concentrations do not vary with height in a layer
248 between the surface and the planetary boundary layer (PBL) top around 1 km in altitude.
249 However, above the PBL top, it is assumed that they decrease exponentially with height,
250 although the shape of size distribution and composition do not change with height. It is
251 assumed that there are no differences in the properties of INP and CCN except for
252 concentrations. It is also assumed that the concentration of aerosols acting as CCN is 100
253 times higher than that acting as INP over grid points at the first time step based on a general
254 difference in concentrations between CCN and INP (Pruppacher and Klett, 1978). Hence,
255 the concentration of aerosols acting as INP at the first time step is 2 cm^{-3} in the control run.
256 This assumed concentration of aerosols acting as INP is higher than usual (Seinfeld and
257 Pandis, 1998). However, Hartmann et al. (2021) observed the INP concentration that was
258 higher than assumed here in the Svalbard area when there were strong dust events, meaning
259 that the assumed INP concentration is not that unrealistic.

260 To examine effects of aerosols on mixed-phase clouds, the control run is repeated by
261 increasing the concentration of aerosols by a factor of 10. In the repeated (control) run, the
262 initial concentrations of aerosols acting as CCN and INP at grid points immediately above
263 the surface are 2000 (200) and 20 (2) cm^{-3} , respectively. Reflecting these concentrations in
264 the simulation name, the control run is referred to as “the 200_2 run” and the repeated run
265 is referred to as “the 2000_20 run”. To isolate effects of aerosols acting as CCN (INP) on
266 mixed-phase clouds, the control run is repeated again by increasing the concentration of
267 aerosols acting as CCN (INP) only but not INP (CCN) by a factor of 10. In this repeated
268 run with the increase in the concentration of aerosols acting as CCN (INP), the initial



269 concentrations of aerosols acting as CCN and IFN at grid points immediately above the
270 surface are 2000 (200) and 2 (20) cm^{-3} , respectively. Reflecting this, the repeated run is
271 referred to as “the 2000_2 (200_20) run”.

272

273 **2.2.2 Additional simulations**

274

275 To isolate impacts of ice processes on the adopted case and its interactions with aerosols,
276 the 200_2 and 2000_2 runs are repeated by removing ice processes. These repeated runs
277 are referred to as the 200_2_noice and 2000_2_noice runs. In the 200_2_noice and
278 2000_2_noice runs, all hydrometeors (i.e., ice crystals, snow, graupel, and hail), phase
279 transitions (e.g., deposition and sublimation) and aerosols (i.e., INP) which are associated
280 with ice processes are removed. Hence, in these runs, only droplets (i.e., cloud liquid),
281 raindrops, associated phase transitions (e.g., condensation and evaporation) and aerosols
282 acting as CCN are present, regardless of temperature. Stated differently, these noice runs
283 simulate the warm-cloud counterpart of the selected mixed-phase cloud system. Via
284 comparisons between a pair of the 200_2 and 2000_2 runs and a pair of the 200_2_noice
285 and 2000_2_noice runs, the role of ice processes in the differentiation between mixed-
286 phase and warm clouds is to be identified. Along with this identification, the role of the
287 interplay between ice crystals and droplets in the development of the selected mixed-phase
288 cloud system and its interactions with aerosols is to be isolated.

289 As detailed in Sections 3.1.2 and 3.2.2 below, the test of ICNC/CDNC as a general
290 factor requires more simulations to see impacts of ICNCavg/CDCNavg on clouds and their
291 interactions with aerosols. Here, ICNCavg (CDNCavg) represents the average ICNC
292 (CDNC) over grid points and time steps with non-zero ICNC (CDNC).
293 ICNCavg/CDNCavg represents overall ICNC/CDNC over the domain and simulation
294 period. To respond to this requirement, 200_2_fac10, 200_2_fac10_CCN10,
295 200_2_fac10_INP10 runs are performed and their details are given in Sections 3.1.2 and
296 3.2.2. The summary of simulations in this study is given in Table 1.

297

298 **3. Results**

299



300 **3.1 The 200_2 run vs. the 200_2_noise run**

301

302 The time- and domain-averaged IWP (IWC) is ~one order of magnitude greater than LWP
303 (LWC) in the 200_2 run (Figure 4 and Table 2). For the sake of simplicity, the averaged
304 IWC (IWP) over the averaged LWC (LWP) is denoted by IWC (IWP)/LWC (LWP),
305 henceforth. IWC/LWC and IWP/LWP are 26.28 and 25.96, respectively, in the 200_2 run.
306 Since IWP and LWP are vertically integrated IWC and LWC over the vertical domain,
307 respectively, the qualitative nature of differences between IWC and LWC is not much
308 different from that between IWP and LWP.

309 To understand process-level mechanisms that control the results, microphysical
310 processes are analyzed. As indicated by Ovchinnikov et al. (2011), in clouds with weak
311 precipitation, there is a high-degree correlation between IWC (IWP) and deposition or
312 between LWC (LWP) and condensation, considering that deposition and condensation are
313 sources of IWC (IWP) and LWC (LWP), respectively. In the 200_2 run, the surface
314 precipitation rate is $\sim 0.0020 \text{ mm hr}^{-1}$, which can be considered weak. Hence, in this case,
315 condensation and deposition are considered proxies for IWC (IWP) and LWC (LWP),
316 respectively. Based on this, to gain a process-level understanding of microphysical
317 processes that control the simulated IWC (IWP) or LWC (LWP), condensation and
318 deposition are analyzed.

319 As seen in Figure 5 and Table 2, the average deposition rate is ~one order of magnitude
320 greater than condensation rate in the 200_2 run, leading to much greater IWC (IWP) than
321 LWC (LWP) in the 200_2 run. This is in contrast to the situation in the case of mixed-
322 phase stratocumulus clouds, which were located in a midlatitude region, in Lee et al. (2022).
323 In this case, the average IWC (IWP) and LWC (LWP) are at the same order of magnitude.
324 For the sake of brevity, this case in Lee et al. (2022) is referred to as “the midlatitude case”,
325 while the case of mixed-phase clouds, which is adopted by this study, in the Svalbard area
326 is referred to “the polar case”, henceforth. In the midlatitude case, IWC/LWC and
327 IWP/LWP are 1.55 and 1.57, respectively, which are ~ one order of magnitude smaller
328 than those in the polar case.

329 Warm clouds in the 200_2_noise run shows that the time- and domain-averaged
330 condensation rate that is lower than the time- and the domain-averaged sum of



331 condensation and deposition rates in the 200_2 run (Figure 5 and Table 2). This leads to a
332 situation where warm clouds in the 200_2_noise run shows the time- and domain-averaged
333 LWC that is lower than the time- and domain-averaged water content (WC), which is the
334 sum of IWC and LWC, in mixed-phase clouds in the 200_2 run (Figure 4 and Table 2).
335 Associated with this, the time- and domain-averaged LWP in the 200_2_noise run is lower
336 than the time- and domain-averaged water path (WP), which is the sum of IWP and LWP,
337 in the 200_2 run (Table 2). This is despite the fact that LWC and LWP in the 200_2_noise
338 run are higher than LWC and LWP, respectively, in the 200_2 run (Figure 4 and Table 2).
339 Here, WC (WP) represents the total cloud mass in mixed-phase clouds, while LWC (LWP)
340 alone represents the total cloud mass in warm clouds. These results are also in contrast to
341 the situation in the midlatitude case. The total cloud mass in warm clouds, which are
342 generated by removing ice processes in the midlatitude case, is greater than that in the
343 midlatitude case.

344 It should be noted that the average rate of sedimentation of droplets over the cloud
345 base and simulation period reduces from the 200_2_noise run to the 200_2 run (Table 2).
346 This is mainly due to the decrease in LWC or LWP from the 200_2_noise run to the 200_2
347 run. The average rate of sedimentation of ice crystals over the cloud base and simulation
348 period increases from the 200_2_noise run to the 200_2 run, since there is no sedimentation
349 of ice crystals in the 200_2_noise run (Table 2). The average entrainment rate over the
350 cloud top and simulation period increases from the 200_2_noise run to the 200_2 run
351 (Table 2). Hence, the droplet sedimentation tends to increase the total cloud mass in the
352 200_2 run, and the ice-crystal sedimentation and entrainment tend to reduce the total cloud
353 mass in the 200_2 run, as compared to that in the 200_2_noise run. This means that the
354 droplet sedimentation contributes to increase in the total cloud mass from the 200_2_noise
355 run to the 200_2 run, while entrainment and the ice-crystal sedimentation counter the
356 increase. Thus, entrainment and the ice-crystal sedimentation should be opted out when it
357 comes to mechanisms leading to the increase in the total cloud mass. Here, the vertical
358 integration of each of condensation and deposition rates is obtained over each cloudy
359 column in the domain for each of the runs. For the sake of the brevity, this vertical
360 integration of condensation (deposition) rate is referred to as the integrated condensation
361 (deposition) rate. Then, each of the integrated condensation and deposition rates is



362 averaged over cloudy columns and the simulation period. It is found that the change in the
363 average rate of the droplet sedimentation over the cloud base and simulation period from
364 the 200_2_noice run to the 200_2 run is ~five to six orders of magnitude smaller than that
365 in the sum of the average integrated condensation rate and the average integrated deposition
366 rate (Table 2). Thus, condensation and deposition, but not the droplet sedimentation, are
367 main factors controlling differences in cloud mass in cloudy columns, which is represented
368 by LWP, IWP, and associated LWC and IWC, and in the total cloud mass between the
369 200_2 and 200_2_noice runs as are between the midlatitude case and its warm-cloud
370 counterpart.

371

372 **3.1.1 Hypothesis**

373

374 We hypothesized that ICNC/CDNC can be an important factor that determines above-
375 described differences between the polar and midlatitude cases. Remember that there are
376 more ice crystals as sources of deposition per a droplet when ICNC/CDNC is higher. Thus,
377 when ICNC/CDNC is higher and $q_v > q_{sw}$, there is a higher possibility that more portion
378 of water vapor is deposited onto ice crystals by stealing water vapor, which is supposed to
379 be condensed onto droplets, from droplets in an air parcel. Here, q_v and q_{sw} represent
380 water-vapor pressure and water-vapor saturation pressure for liquid water or droplets,
381 respectively. When ICNC/CDNC is higher and $q_{si} < q_v < q_{sw}$, there are more ice crystals
382 that can absorb water vapor, including that which is produced by droplet evaporation, per
383 a droplet; here, q_{si} represents water-vapor saturation pressure for ice water or ice crystals.
384 Thus, with higher ICNC/CDNC, there is a higher possibility that more portion of water
385 vapor is deposited onto ice crystals in an air parcel as shown in Lee et al. (2022).

386 ICNC_{avg}/CDNC_{avg} is 0.22 in the control run (i.e., the 200_2 run) for the polar case
387 and 0.019 in the control run for the midlatitude case which is described in Lee et al. (2022).
388 Henceforth, the control run for the midlatitude case is referred to as the control-midlatitude
389 run. ICNC_{avg}/CDNC_{avg} is ~one order of magnitude higher for the polar case than for the
390 midlatitude case. This is despite the fact that the ratio of the initial number concentration
391 of aerosols acting as INP to that of acting as CCN is identical between the 200_2 and
392 control-midlatitude runs. This is mainly due to the fact that ice nucleation strongly depends



393 on air temperature (Prappucher and Klett, 1978). When supercooling is stronger, in general,
394 there is more nucleation of ice crystals for a given group of aerosols acting as INP. The
395 average air temperature immediately below the cloud base over the simulation period is -
396 16 °C in the 200_2 run and -5 °C in the control-midlatitude run. The average air temperature
397 immediately above the cloud top is -33 °C in the 200_2 run and -15 °C in the control-
398 midlatitude run. Hence, there is more supercooling which contributes to the higher
399 ICNCavg/CDNCavg in the polar case than in the midlatitude case. The higher
400 ICNCavg/CDNCavg is likely to induce more portion of water vapor to be deposited onto
401 ice crystals in the polar case than in the midlatitude case. It is hypothesized that this in turn
402 enables IWC/LWC or IWP/LWP in the 200_2 run to be one order of magnitude greater
403 than that in the control-midlatitude run. Higher IWC/LWC (IWP/LWP) results in WC (WP)
404 in the 200_2 run which is greater than LWC (LWP) in the warm clouds in the 200_2_noice
405 run, while lower IWC/LWC (IWP/LWP) results in WC (WP) in the midlatitude mixed-
406 phase clouds which is lower than LWC (LWP) in their warm-cloud counterpart. This
407 means that with higher ICNC/CDNC, IWC/LWC and IWP/LWP, ice processes enhance
408 the total cloud mass for the polar case as compared to that for the polar warm-cloud
409 counterpart. However, in the midlatitude case, with lower ICNC/CDNC, IWC/LWC and
410 IWP/LWP, ice processes reduce the total cloud mass as compared to that for the midlatitude
411 warm-cloud counterpart.

412

413 **3.1.2 Role of ICNC/CDNC**

414

415 To test the hypothesis above about the role of ICNC/CDNC in above-described differences
416 between the polar and midlatitude cases, the 200_2 run is repeated by reducing
417 ICNCavg/CDNCavg by a factor of 10. This is done by reducing the concentration of
418 aerosols acting as INP but not CCN in a way that ICNCavg/CDNCavg is lower by a factor
419 of 10 in the repeated run than in the 200_2 run. In this way, this repeated run has
420 ICNCavg/CDNCavg at the same order of magnitude as that in the control-midlatitude run.
421 This repeated run is referred to as the 200_2_fac10 run. As shown in Figure 6 and Table 2,
422 the 200_2_fac10 run shows much lower deposition rate, IWC and IWP than the 200_2 run
423 does. However, as we move from the 200_2 run to the 200_2_fac10 run, the time- and



424 domain-averaged condensation rate, LWC and LWP increases (Figure 6 and Table 2). This
425 is because reduction in deposition increases the amount of water vapor, which is not
426 consumed by deposition but available for condensation. Associated with this, in the
427 200_2_fac10 run, the time- and domain-averaged deposition rate, IWC and IWP become
428 similar to the average condensation rate, LWC and LWP, respectively (Figure 6 and Table
429 2). Hence, IWC/LWC and IWP/LWP reduce from 26.28 and 25.96 in the 200_2 run to 1.05
430 and 1.02, respectively, in the 200_2_fac10 run. Here, IWC/LWC and IWP/LWP in the
431 200_2_fac10 run are similar to those in the midlatitude-control run, which demonstrate that
432 the difference in ICNC/CDNC is able to explain the difference in IWC/LWC and
433 IWP/LWP between the polar and midlatitude cases. It is notable that the reduction in
434 deposition is dominant over the increase in condensation with the decrease in
435 ICNCavg/CDNCavg. Hence, the sum of condensation and deposition rates, WC and WP
436 reduce from the 200_2 run to the 200_2_fac10 run. It is also notable that the sum of
437 condensation and deposition rates, WC and WP reduce in a way that the sum, WC and WP
438 in the mixed-phase clouds in the 200_2_fac10 run are lower than condensation rate, LWC
439 and LWP in the warm clouds in the 200_2_noice run, respectively (Figure 6 and Table 2).
440 This is similar to the situation in the midlatitude case and thus demonstrates that the
441 different relation between the mixed-phase and warm clouds can be explained by the
442 difference in ICNC/CDNC between the polar and midlatitude cases.

443 The rate of the sedimentation of ice crystals at the cloud base reduces as
444 ICNCavg/CDNCavg reduces between the 200_2 and 200_2_fac10 runs, mainly due to
445 reduction in the ice-crystal mass (Table 2). The rate of droplet sedimentation at the cloud
446 base increases as ICNCavg/CDNCavg reduces mainly due to increases in droplet mass and
447 size in association with the increases in LWC and LWP (Table 2). The entrainment rate at
448 the cloud top reduces as ICNCavg/CDNCavg reduces (Table 2). Hence, the changing
449 sedimentation tends to reduce LWC or LWP and increase IWC or IWP, while the changing
450 entrainment tends to increase the total cloud mass, WC or WP with the reducing
451 ICNCavg/CDNCavg. Hence, changes in the sedimentation counter the increase in LWC or
452 LWP, and the decrease in IWC or IWP with the reducing ICNCavg/CDNCavg. Changes
453 in the entrainment counters the decrease in WC or WP with the reducing
454 ICNCavg/CDNCavg between the 200_2 and 200_2_fac10 runs. Here, we see that changes



455 in the sedimentation and entrainment are not factors that lead to the increase in LWC or
456 LWP, and the decrease in IWC or IWP, and eventually the decrease in WP with the
457 reducing ICNCavg/CDNCavg. The analysis of the sedimentation and entrainment exclude
458 them from factors inducing above-described differences between the 200_2 and
459 200_2_fac10 runs. Instead, this analysis grants more confidence in the fact that deposition
460 and condensation, which are strongly dependent on ICNC/CDNC, are main factors
461 inducing those differences.

462

463 **3.2 Aerosol-cloud interactions**

464

465 Comparisons between the 200_2 and 2000_20 runs show that with the increasing
466 concentration of both of aerosols acting as CCN and those as INP, there are increases in
467 IWC and IWP but decreases in LWC and LWP in the polar case (Figures 7 and Table 2).
468 These decreases in LWC and LWP are negligible as compared to these increases in IWC
469 and IWP. Hence, the increases in IWC and IWP outweigh the decreases in LWC and LWP,
470 leading to aerosol-induced increases in WC and WP, respectively (Figures 7 and Table 2).
471 To identify roles of specific types of aerosols in these aerosol-induced changes,
472 comparisons not only between the 200_2 and 200_20 runs but also between the 200_2 and
473 2000_2 runs are performed. Comparisons between the 200_2 and 200_20 runs show that
474 the increasing concentration of aerosols acting as INP induces increases in IWC and IWP
475 but decreases in LWC and LWP (Figure 7 and Table 2). The magnitudes of these increases
476 and decreases are similar to those between the 200_2 and 2000_20 runs (Figure 7 and Table
477 2). However, comparisons between the 200_2 and 2000_2 runs show that the increasing
478 concentration of aerosols acting as CCN induces negligible changes in either a pair of IWC
479 and IWP or a pair of LWC and LWP. Thus, there are negligible CCN-induced changes in
480 the total cloud mass, although the increasing concentration of aerosols acting as CCN
481 induces a slight decrease in IWC and IWP, and a slight increase in LWC and LWP (Figure
482 7 and Table 2). This demonstrates that INP plays a much more important role than CCN
483 when it comes to the response of the liquid, ice and total cloud mass to increasing aerosol
484 concentrations. However, in the midlatitude case, the increasing concentration of aerosols



485 acting as CCN generates changes in the mass as significantly as the increasing
486 concentration of aerosols acting as INP does.

487 To identify roles played by ice processes in aerosol-cloud interactions, a pair of the
488 200_2_noise and 2000_2_noise runs are analyzed and compared to the previous four
489 standard simulations (i.e., the 200_2, 200_20, 2000_2 and 2000_20 runs). The CCN-
490 induced increases in LWC and LWP in those noise runs are much greater than the CCN-
491 induced changes in WC and WP, respectively, in the 200_2 and 2000_2 runs (Figure 7 and
492 Table 2). However, these CCN-induced increases in LWC and LWP in the noise runs are
493 smaller than the INP-induced increases in WC and WP, respectively, in the 200_2 and
494 200_20 runs. This is different from the midlatitude case where changes in the total cloud
495 mass, whether they are induced by the increasing concentration of aerosols acting as CCN
496 or INP, in the mixed-phase clouds are much lower than those CCN-induced changes in the
497 warm clouds.

498

499 **3.2.1 Deposition, condensation, sedimentation and entrainment**

500

501 There are the CCN-induced negligible increases (decreases) in condensation (deposition)
502 rate, leading to the CCN-induced negligible increases (decreases) in LWC and LWP (IWC
503 and IWP) between the 200_2 and 2000_2 runs (Figure 7 and Table 2). However, between
504 the 200_2 and 200_20 runs, there are rather the significant INP-induced increases in
505 deposition rate, leading to the significant INP-induced increases in IWC and IWP (Figure
506 7 and Table 2). Between the 200_2 and 200_20 runs, there are negligible INP-induced
507 decreases in condensation rate, leading to the negligible INP-induced decreases in LWC
508 and LWP, as compared to the INP-induced increases in deposition rate, IWC and IWP
509 (Figure 7 and Table 2). With the increasing concentration of aerosols acting as INP from
510 the 200_2 run to the 200_20 run, there are decreases in the sedimentation of ice crystals at
511 the cloud base (Table 2). This is mainly due to decreases in the size of ice crystals in
512 association with increases INP and resultant increases in ICNC. From the 200_2 run to the
513 200_20 run, there are decreases in the sedimentation of droplets at the cloud base as shown
514 in Table 2, mainly due to decreases in LWC or LWP. From the 200_2 run to the 200_20
515 run, there are increases in the entrainment at the cloud top (Table 2). Hence, the INP-



516 induced changes in the sedimentation contribute to the INP-induced increases in IWC or
517 IWP but counter the INP-induced reduction in LWC or LWP. The entrainment counters
518 the INP-induced increases in WC or WP. Hence, we see that changes in entrainment and
519 the droplet sedimentation are not factors that lead to the INP-induced increases in WC (WP)
520 and decreases in LWC (LWP), respectively. The INP-induced increases in deposition and
521 decreases in the sedimentation of ice crystals both contribute to the INP-induced increases
522 in IWC and IWP. However, the INP-induced changes in the average integrated deposition
523 rate over cloudy columns and the simulation period is \sim four orders of magnitude greater
524 than those in the average rate of ice-crystal sedimentation at the cloud base and simulation
525 period (Table 2). Hence, the role of the ice-crystal sedimentation in the INP-induced
526 changes in IWC and IWP is negligible as compared to that of deposition.

527 In the warm clouds in the 200_2_noice and 2000_2_noice runs, there are the CCN-
528 induced increases in condensation rate, leading to those in LWC and LWP (Figure 7 and
529 Table 2). However, the CCN-induced increases in condensation rate in the warm clouds
530 associated with the polar case are lower than the INP-induced increases in deposition rate
531 in the polar case (Table 2). This contributes to aerosol-induced smaller changes in the total
532 cloud mass in the polar warm clouds than in the polar mixed-phase clouds. The
533 sedimentation of droplets at the cloud base reduces and the entrainment at the cloud top
534 increases from the 200_2_noice run to 2000_2_noice run (Table 2). The increasing
535 concentration of aerosols acting as CCN induces increases in CDNC and decreases in the
536 droplet size, leading to the reduction in the droplet sedimentation from the 200_2_noice
537 run to 2000_2_noice run. The CCN-induced changes in the sedimentation contribute to the
538 CCN-induced increases in LWC and LWP. The entrainment counters the CCN-induced
539 increases in LWC or LWP. Hence, the entrainment is not a factor which induces the CCN-
540 induced increases in LWC or LWP between the 200_2_noice and 2000_2_noice runs. As
541 seen in Table 2, the CCN-induced changes in the sedimentation rate are \sim three orders of
542 magnitude smaller than those in the integrated condensation rate. Hence, the role of
543 sedimentation in changes in LWP or WP between the 200_2_noice and 2000_2_noice runs
544 is negligible as compared to that of condensation.

545

546 **3.2.2 Understanding differences between the polar and midlatitude cases**



547

548 Roughly speaking, the CCN-(INP)-induced changes in LWC (IWC) or LWP (IWP) via
549 CCN-(INP)-induced changes in autoconversion of droplets (ice crystals) are proportional
550 to LWC (IWC) or LWP (IWP) that changing CCN (INPs) affect (e.g., Liu and Daum (2004);
551 Kogan (2013); Lee and Baik (2017); Dudhia, 1989; Lim and Hong, 2010; Mansell et al.
552 2010). This is for given environmental conditions (e.g., temperature and humidity) and
553 given CCN-(INP)-induced changes in microphysical factors such as sizes and number
554 concentrations of droplets (ice crystals). Hence, in the polar case, with a given much lower
555 LWC (LWP) than IWC (IWP), the changing concentration of aerosols acting as CCN is
556 likely to induce smaller changes in the given LWC (LWP) via CCN impacts on the droplet
557 autoconversion. This is as compared to changes in the given IWC or IWP which are
558 induced by the changing concentration of aerosols acting as INP and thus changing ice-
559 crystal autoconversion.

560 The smaller (larger) changes in the given LWC or LWP (IWC or IWP) are related to
561 changes in CDNC (ICNC), which are initiated by those in droplet (ice crystal)
562 autoconversion, and associated integrated droplet (ice-crystal) surface area. Remember that
563 condensation (deposition) occurs on droplet (ice-crystal) surface and thus droplets (ice
564 crystals) act as a source of condensation (deposition). Hence, those changes in CDNC
565 (ICNC) and integrated droplet (ice-crystal) surface area can lead to changes in
566 condensation (deposition) and thus feedbacks between condensation (deposition) and
567 updrafts. The smaller CCN-induced changes in LWC or LWP involve changes in CDNC
568 and associated smaller changes in condensation and associated feedbacks between
569 condensation and updrafts in the polar case. This is as compared to changes in deposition
570 and feedbacks between deposition and updrafts which are associated with the INP-induced
571 changes in ICNC and the related larger INP-induced changes in IWC and IWP in the polar
572 case. The smaller CCN-induced changes in LWC (or LWP) involve smaller changes in
573 water vapor that is consumed by droplets in the polar case. The larger INP-induced changes
574 in IWC (or IWP) involve larger changes in water vapor that is consumed by ice crystals in
575 the polar case. This leaves the CCN-induced smaller changes in the amount of water vapor
576 available for deposition, which induce the smaller CCN-induced changes in IWC and IWP
577 in the polar case. This is as compared to the INP-induced changes in the amount of water



578 vapor which is available for condensation and associated changes in LWC or LWP in the
579 polar case. The lower LWC (LWP) in the polar warm clouds than IWC (IWP) in the polar
580 case contributes to the INP-induced greater changes in IWC (IWP) than the CCN-induced
581 changes in LWC (LWP) in the polar warm clouds. The lower LWC (LWP) in the polar
582 case than that in the polar warm clouds contributes to the CCN-induced greater changes in
583 LWC (LWP) in the polar warm clouds than those in LWC (LWP) and subsequent changes
584 in IWC (IWP) in the polar case.

585 In contrast to the situation in the polar case, in the midlatitude case, remember that a
586 given LWC (LWP) is at the same order of magnitude of IWC (IWP). Hence, the CCN-
587 induced changes in LWC (LWP) and subsequent changes in IWC (IWP) are similar to the
588 INP-induced changes in IWC (IWP) and subsequent changes in LWC (LWP). The greater
589 LWC (LWP) in the midlatitude warm cloud than both of LWC (LWP) and IWC (IWP) in
590 the midlatitude case contributes to the greater CCN-induced changes in LWC (LWP) in the
591 midlatitude warm cloud. This is as compared to either the CCN-induced changes in LWC
592 (LWP) and subsequent changes in IWC (IWP) or the INP-induced changes in IWC (IWP)
593 and subsequent changes in LWC (LWP) in the midlatitude case.

594 To confirm above-described mechanisms in this section, which explain different
595 aerosol-cloud interactions between the polar and midlatitude cases, the 200_2_fac10 run is
596 repeated by increasing INP by a factor of 10 in the PBL at the first time step. This repeated
597 run is referred to as “the 200_2_fac10_INP10 run. Then, the 200_2_fac10 run is repeated
598 again by increasing CCN by a factor of 10 in the PBL at the first time step. This repeated
599 run is referred to as the 200_2_fac10_CCN10 run. These repeated runs are to see the
600 response of IWC, IWP, LWC and LWP to the increasing concentration of aerosols acting
601 as INP and CCN. This is when IWC (IWP) and LWC (LWP) are at the same order of
602 magnitude and lower in mixed-phase clouds than LWC (LWP) in the warm-cloud
603 counterpart as in the 200_2_fac10 run and midlatitude case. Comparisons between the
604 200_2_fac10, 200_2_fac10_INP10 and 200_2_fac10_CCN10 runs show that the INP-
605 induced changes in IWC (IWP) and LWC (LWP) are at the same order of magnitude of the
606 CCN-induced changes in IWC (IWP) and LWC (LWP), respectively, as in the midlatitude
607 case. These comparisons also show that the CCN-induced changes in LWC (LWP) in the
608 polar warm cloud are greater. This is as compared to either the CCN-induced changes in



609 LWC (LWP) and subsequent changes in IWC (IWP) between the 200_2_fac10 and
610 200_2_fac10_CCN10 runs or the INP-induced changes in IWC (IWP) and subsequent
611 changes in LWC (LWP) between the 200_2_fac10 and 200_2_fac10_INP10 runs. These
612 comparisons demonstrate that differences in ICNC/CDNC play a critical role in differences
613 in aerosol-cloud interactions between the polar and midlatitude cases, considering that
614 differences in ICNC/CDNC between the 200_2 and 200_2_fac10 runs are at the same order
615 of magnitude of that between the cases.

616

617 **5. Summary and conclusions**

618

619 In this study, a case of mixed-phase clouds in a polar area, which is referred to as “the polar
620 case” is compared to that in a midlatitude area, which is referred to as “the midlatitude
621 case”. This is to gain an understanding of how different ICNC/CDNC plays a role in
622 making differences in cloud properties, their interactions with aerosols and impacts of ice
623 processes on them between two representative areas (i.e., polar and midlatitude areas)
624 where mixed-phase stratiform clouds form and develop. Among those cloud properties,
625 this study focuses on is IWC/LWC or IWP/LWP that plays an important role in cloud
626 radiative properties.

627 Due to lower air temperature, more ice crystals are nucleated, leading to higher
628 ICNC/CDNC in the polar case than in the midlatitude case. This higher ICNC/CDNC
629 enables the more efficient deposition of water vapor onto ice crystals in the polar case. This
630 leads to much higher IWC/LWC or IWP/LWP in the polar case. The more efficient
631 deposition of water vapor onto ice crystals enables the polar mixed-phase clouds to have
632 the greater total cloud mass than the polar warm clouds. However, the less efficient
633 deposition of water vapor onto ice crystals causes the midlatitude mixed-phase clouds to
634 have less total cloud mass than the midlatitude warm clouds. With the increasing
635 ICNC/CDNC from the midlatitude case to the polar case, impacts of CCN (IFN) on the
636 total cloud mass become less (more) important.

637 This study picked ICNC/CDNC, which is affected by air temperature and its impacts
638 on ice-crystal nucleation, as an important factor which differentiates interactions among
639 cloud properties, aerosols and ice processes in the polar area from those in the midlatitude



640 area. Differences in ICNC/CDNC initiate differences in the microphysical properties (e.g.,
641 the integrated surface area), and then, subsequently induce those in thermodynamic latent-
642 heat processes (e.g., condensation and deposition), dynamics of clouds and interactions
643 among clouds, aerosols and ice processes. However, this does not mean that there are no
644 other potential factors which can explain the variation of cloud properties and interactions
645 among those properties, aerosols and ice processes between those areas. For example,
646 differences in environmental factors (e.g., stability and wind shear) between the areas can
647 have impact on the variation. Particularly, differences in stability and wind shear can
648 initiate those in the dynamic development of turbulence. Then, this subsequently induces
649 differences in the microphysical and thermodynamic development of clouds and
650 interactions among clouds, aerosols and ice processes. Hence, factors such as stability and
651 wind shear can have different orders of procedures, which involve dynamics,
652 thermodynamics and microphysics, than ICNC/CDNC in terms of differentiation between
653 the polar and midlatitude mixed-phase clouds. Thus, different mechanisms controlling the
654 differentiation can be expected regarding factors such as stability and wind shear as
655 compared to ICNC/CDNC. The examination of these different mechanisms among
656 stability, wind shear and ICNC/CDNC deserves future study for more comprehensive
657 understanding of the differentiation.

658 Another point to make is that the cases in this study have weak precipitation and the
659 associated weak sedimentation of ice crystals and droplets. In mixed-phase clouds with
660 strong precipitation and the sedimentation, they can play roles as important as in-cloud
661 latent-heat processes in cloud development, interactions among clouds, aerosols and ice
662 processes, and their variation among different cases of mixed-phase clouds. Hence, in those
663 clouds with strong precipitation, the sedimentation can take part in the interplay between
664 ICNC/CDNC and latent-heat processes, and play a role in the differentiation of cloud
665 properties and interactions among those properties, aerosols and ice processes when it
666 comes to different cases of mixed-phase clouds. For more generalization of results here,
667 this potential role of sedimentation needs to be investigated by performing more case
668 studies involving cases with strong precipitation in the future.

669 It should be emphasized that although this study mentions air temperature as a factor
670 that affects ICNC/CDNC, ICNC/CDNC can be affected by other factors such as sources of



671 aerosols acting as INP and those acting as CCN, and/or the advection of those aerosols.
672 Hence, even for cloud systems that develop with a similar air-temperature condition, for
673 example, when those systems are affected by different sources of aerosols and/or their
674 advection, they are likely to have different ICNC/CDNC, IWP/LWP and relative
675 importance of impacts of INP and CCN on IWP and LWP.

676 This study suggests that differences in IWP/LWP and the relative importance of the
677 impacts of INP and CCN on IWP and LWP among different systems of stratocumulus
678 clouds can be explained by a microphysical factor, which is ICNC/CDNC. This factor can
679 be a simplified and useful tool to understand differences among those different systems in
680 terms of IWP/LWP and the relative importance of INP and CCN in aerosol-cloud
681 interactions. This factor can also be a useful tool for a simplified understanding of different
682 roles of ice processes when mixed-phase clouds are compared to their warm-cloud
683 counterparts in terms of the cloud development and its interactions with aerosols among
684 those different systems. It should be noted that warm clouds have been studied much more
685 than mixed-phase clouds, although mixed-phase clouds play as important roles as warm
686 clouds in the evolution of climate and its change. This study provides preliminary
687 mechanisms which differentiate mixed-phase clouds and their interactions with aerosols
688 from their warm-cloud counterparts as a way of improving our understanding of mixed-
689 phase clouds. It should be mentioned that the efficient way of developing general
690 parameterizations, which are for climate models and consider all of warm, mixed-phase
691 clouds and their interactions with aerosols, can be achieved by just adding those
692 mechanisms to pre-existing parameterizations of warm clouds instead of developing brand
693 new parameterizations from the scratch. Hence, although those mechanisms identified in
694 this study may not be complete, they can act as a valuable building block that can
695 streamline the development of general parameterizations.

696
697
698
699
700
701



702 **Code/Data source and availability**

703

704 Our private computer system stores the code/data which are private and used in this study.

705 Upon approval from funding sources, the data will be opened to the public. Projects related

706 to this paper have not been finished, thus, the sources prevent the data from being open to

707 the public currently. However, if information on the data is needed, contact the

708 corresponding author Seoung Soo Lee (slee1247@umd.edu).

709

710 **Author contributions**

711 Essential initiative ideas are provided by SSL, CHJ and YJY to start this work. Simulation

712 and observation data are analyzed by SSL, CHJ and JU. YZ, JP, MGM and SKS review

713 the results and contribute to their improvement.

714

715 **Competing interests**

716 The authors declare that they have no conflict of interest.

717

718 **Acknowledgements**

719 This study is supported by the National Research Foundation of Korea (NRF) grant funded

720 by the Korea government (MSIT) (Nos. NRF2020R1A2C1003215,

721 NRF2023R1A2C1002367, NRF2021M1A5A1065672/KOPRI-PN23011 and

722 2020R1A2C1013278), the Korea Meteorological Administration Research and

723 Development Program "Research on Weather Modification and Cloud Physics" under

724 Grant (KMA2018-00224) and Basic Science Research Program through the NRF funded

725 by the Ministry of Education (No. 2020R1A6A1A03044834).

726

727

728

729

730

731

732

733

734

735

736 **References**

737

738 Albrecht, B. A.: Aerosols, cloud microphysics, and fractional cloudiness, *Science*, 245,
739 1227-1230, 1989.

740 Bartosiewicz, Y., and Duponcheel, M.: Large eddy simulation: Application to liquid metal
741 fluid flow and heat transfer . In: Roelofs, Ferry, *Thermal Hydraulics Aspects of Liquid*
742 *Metal Cooled Nuclear Reactors*, Woodhead Publishing, 2018.

743 Brown, A., Milton, S., Cullen, M., Golding, B., Mitchell, J., and Shelly, A.: Unified
744 modeling and prediction of weather and climate: A 25-year journey, *B. Am. Meteorol.*
745 *Soc.*, 93, 1865–1877, 2012.

746 Chen, F., and Dudhia, J.: Coupling an advanced land-surface hydrology model with the
747 Penn State-NCAR MM5 modeling system. Part I: Model description and
748 implementation, *Mon. Wea. Rev.*, 129, 569–585, 2001.

749 Choi, Y.-S., Ho, C.-H., Park, C.-E., Storelvmo, T., and Tan, I.: Influence of cloud phase
750 composition on climate feedbacks, *J. Geophys. Res.*, 119, 3687–3700,
751 doi:10.1002/2013JD020582, 2014.

752 Choi, Y.-S., Lindzen, R. S., Ho, C.-H., and Kim, J.: Space observations of cold-cloud phase
753 change, *Proc. Natl. Acad. Sci. U.S.A.*, 107, 11211–11216, 2010

754 Chua, X. R., and Ming, Y.: Convective invigoration traced to warm-rain microphysics,
755 *Geophys. Res. Lett.*, 47, <https://doi.org/10.1029/2020GL089134>, 2020.

756 Dione, C., Lohou, F., Lothon, M., Adler, B., Babić, K., Kalthoff, N., Pedruzo-Bagazgoitia,
757 X., Bezombes, Y., and Gabella, O.: Low-level stratiform clouds and dynamical
758 features observed within the southern West African monsoon, *Atmos. Chem. Phys.*,
759 19, 8979–8997, <https://doi.org/10.5194/acp-19-8979-2019>, 2019.

760 Dudhia, J., Numerical study of convection observed during the winter monsoon
761 Experiment using a mesoscale two-dimensional Model, *J. Atmos. Sci.*, 46, 3077–3107,
762 <https://doi.org/10.1175/1520-0469>, 1989.

763 Fan, J., Rosenfeld, D., Zhang, Y., Giangrande, S. E., Li, Z., Machado, L. A. T., Martin, S.
764 T., Yang, Y., Wang, J., and Artaxo, P.: Substantial convection and precipitation
765 enhancements by ultrafine aerosol particles. *Science*, 359, 411–418, 2018

766 Forster, P., et al., Changes in atmospheric constituents and in radiative forcing, in: *Climate*



- 767 change 2007: the physical science basis, Contribution of working group I to the Fourth
768 Assessment Report of the Intergovernmental Panel on Climate Change, edited by
769 Solomon, S., et al., Cambridge Univ. Press, New York, 2007.
- 770 Hahn, C. J., and Warren, S. G.: A gridded climatology of clouds over land (1971–96) and
771 ocean (1954–97) from surface observations worldwide, Numeric Data Package NDP-
772 026EORNL/CDIAC-153, CDIAC, Department of Energy, Oak Ridge, TN, 2007.
- 773 Hannak, L., Knippertz, P., Fink, A. H., Kniffka, A., and Pante, G.: Why do global climate
774 models struggle to represent low-level clouds in the West African summer monsoon?,
775 *J. Climate*, 30, 1665–1687, <https://doi.org/10.1175/JCLI-D-16-0451.1>, 2017
- 776 Hartmann, D. L., Ockert-Bell, M. E., and Michelsen, M. L.: The effect of cloud type on
777 earth’s energy balance—Global analysis, *J. Climate*, 5, 1281–1304, 1992.
- 778 Hartmann, M., Gong, X., Kecorius, S., van Pinxteren, M., Vogl, T., Welti, A., Wex, H.,
779 Zeppenfeld, S., Herrmann, H., Wiedensohler, A., and Stratmann, F.: Terrestrial or
780 marine – indications towards the origin of ice-nucleating particles during melt season
781 in the European Arctic up to 83.7° N, *Atmos. Chem. Phys.*, 21, 11613–11636,
782 <https://doi.org/10.5194/acp-21-11613-2021>, 2021.
- 783 IPCC: Climate Change: The Physical Science Basis. Contribution of Working Group I to
784 the Sixth Assessment Report of the Intergovernmental Panel on Climate Change
785 [Masson-Delmotte, V., Zhai, P., Pirani, A., Connors, S. L., Péan, C., Berger, S., Caud,
786 N., Chen, Y., Goldfarb, L., Gomis, M. I., Huang, M., Leitzell, K., Lonnoy, E.,
787 Matthews, J. B. R., Maycock, T. K., Waterfield, T., Yelekçi, O., Yu, R., and Zhou, B.
788 (eds.)]. Cambridge University Press, Cambridge, United Kingdom and New York, NY,
789 USA, In press, doi:10.1017/9781009157896, 2021.
- 790 Jung, C. H., Yoon, Y. J., Kang, H. J., Gim, Y., Lee, B. Y., Ström, J., Krejci, R., and Tunved,
791 P.: The seasonal characteristics of cloud condensation nuclei (CCN) in the arctic lower
792 troposphere, *Tellus B: Chemical and Physical Meteorology*, 70:1, 1513291, [https://doi:](https://doi.org/10.1080/16000889.2018.1513291)
793 [10.1080/16000889.2018.1513291](https://doi.org/10.1080/16000889.2018.1513291), 2018.
- 794 Khain, A. P., Ovchinnikov, M., Pinsky, M., Pokrovsky, A. and Krugliak, H.: Notes on the
795 state-of-the-art numerical modeling of cloud microphysics, *Atmos. Res.*, 55, 159–224,
796 2000.
- 797 Khain, A., Pokrovsky, A., Rosenfeld, D., Blahak, U., and Ryzhkoy, A.: The role of CCN in



- 798 precipitation and hail in a mid-latitude storm as seen in simulations using a spectral
799 (bin) microphysics model in a 2D dynamic frame, *Atmos. Res.*, 99, 129–146, 2011.
- 800 Khain, A. P., Phillips, V., Benmoshe, N., Pokrovsky, A.: The role of small soluble aerosols
801 in the microphysics of deep maritime clouds, *J. Atmos. Sci.*, 69, 2787–2807, 2012.
- 802 Knippertz, P., Fink, A. H., Schuster, R., Trentmann, J., Schrage, J. M., and Yorke, C.: Ultra-
803 low clouds over the southern West African monsoon region, *Geophys. Res. Lett.*, 38,
804 L21808, <https://doi.org/10.1029/2011GL049278>, 2011.
- 805 Kogan, Y., 2013: A cumulus cloud microphysics parameterization for cloud-resolving
806 models, *J. Atmos. Sci.*, 70, 1423–1436, <https://doi:10.1175/JAS-D-12-0183.1>, 2013.
- 807 Koop, T., Luo, B. P., Tsias, A., and Peter, T.: Water activity as the determinant for
808 homogeneous ice nucleation in aqueous solutions, *Nature*, 406, 611–614.
- 809 Lee, H., and Baik, J.-J.: A physically based autoconversion parameterization, *J. Atmos. Sci.*,
810 74, 1599–1616, <https://doi.org/10.1175/JAS-D-16-0207.1>, 2017.
- 811 Lee S. S., Penner, J. E., and Saleeby, S. M.: Aerosol effects on liquid-water path of thin
812 stratocumulus clouds, *J. Geophys. Res.*, 114, D07204, doi:10.1029/2008JD010513,
813 2009.
- 814 Lee, S. S., et al., Mid-latitude mixed-phase stratocumulus clouds and their interactions with
815 aerosols: how ice processes affect microphysical, dynamic and thermodynamic
816 development in those clouds and interactions?, *Atmos. Chem. Phys.*,
817 <https://doi.org/10.5194/acp-21-16843-2021>, 2022.
- 818 Li, J., Carlson, B. E., Yung, Y. L., Lv, D., Hansen, J., Penner, J. E., Liao, H., Ramaswamy,
819 V., Kahn, R. A., Zhang, P., Dubovik, O., Ding, A., Lacis, A. A., Zhang, L., and Dong,
820 Y.: Scattering and absorbing aerosols in the climate system, *Nature Reviews Earth and*
821 *Environment*, 3, 363–379, <https://doi.org/10.1038/s43017-022-00296-7>, 2022.
- 822 Lilly, D. K.: The representation of small scale turbulence in numerical simulation
823 experiments, *Proc. Ibm Sci. Comput. Symp. Environ. Sci.*, 320–1951, 195–210, 1967.
- 824 Lim, K.-S. S., and Hong, S.-Y.: Development of an effective double-moment cloud
825 microphysics scheme with prognostic cloud condensation nuclei (CCN) for weather
826 and climate models, *Mon. Wea. Rev.*, 138, 1587–1612,
827 doi:10.1175/2009MWR2968.1., 2010.
- 828 Liu, Y., and Daum, P. H.: Parameterization of the autoconversion. Part I: Analytical



- 829 formulation of the Kessler-type parameterizations, *J. Atmos. Sci.*, 61, 1539–1548,
830 doi:10.1175/1520-0469(2004)061,1539:POTAPI.2.0.CO;2, 2004.
- 831 Lohmann, U. and Diehl, K.: Sensitivity studies of the importance of dust ice nuclei for
832 the indirect aerosol effect on stratiform mixed-phase clouds, *J. Atmos. Sci.*, 63, 968-
833 982, 2006.
- 834 Mansell, E. R., Ziegler, C. L. and Bruning, E. C., Simulated electrification of a small
835 thunderstorm with two-moment bulk microphysics, *J. Atmos. Sci.*, 67, 171–194,
836 doi:10.1175/2009JAS2965.1., 2010.
- 837 Ming, Y., and Chua, X. R.: Convective invigoration traced to warm-rain microphysics,
838 *Geophys. Res. Lett.*, 47, doi.org/10.1029/2020GL089134, 2020.
- 839 Mlawer, E. J., Taubman, S. J., Brown, P. D., Iacono, M. J., and Clough, S. A.: RRTM, a
840 validated correlated-k model for the longwave, *J. Geophys. Res.*, 102, 16663-1668,
841 1997.
- 842 Möhler, O., et al, Efficiency of the deposition mode ice nucleation on mineral dust particles,
843 *Atmos. Chem. Phys.*, 6, 3007-3021, 2006.
- 844 Ovchinnikov, M., Korolev, A., and Fan, J.: Effects of ice number concentration on
845 dynamics of a shallow mixed-phase stratiform cloud, *J. Geophys. Res.*, 116, D00T06,
846 doi:10.1029/2011JD015888, 2011.
- 847 Pruppacher, H. R. and Klett, J. D.: *Microphysics of clouds and precipitation*, 714pp, D.
848 Reidel, 1978.
- 849 Ramaswamy, V., et al.: Radiative forcing of climate change, in *Climate Change 2001: The*
850 *Scientific Basis*, edited by J. T. Houghton et al., 349-416, Cambridge Univ. Press,
851 New York, 2001.
- 852 Smagorinsky, J.: General circulation experiments with the primitive equations, *Mon. Wea.*
853 *Rev.*, 91, 99–164, 1963.
- 854 Stevens, B., and Feingold, G.: Untangling aerosol effects on clouds and precipitation in a
855 buffered system, *Nature*, 461, 607–613, <https://doi.org/10.1038/nature08281>, 2009.
- 856 Stephens, G. L., and Greenwald, T. J.: Observations of the Earth’s radiation budget in
857 relation to atmospheric hydrology. Part II: Cloud effects and cloud feedback, *J.*
858 *Geophys. Res.*, 96, 15 325–15 340, 1991.
- 859 Tunved, P., Ström, J. and Krejci, R.: Arctic aerosol life cycle: linking aerosol size



860 distributions observed between 2000 and 2010 with air mass transport and
861 precipitation at Zeppelin station, Ny-Ålesund, Svalbard, *Atmos. Chem. Phys.*,
862 13, 3643–3660, <https://doi:10.5194/acp-13-3643-2013>, 2013

863 Twomey, S.: Pollution and the Planetary Albedo, *Atmos. Env.*, 8,1251-1256, 1974.

864 Warren, S. G., Hahn, C. J., London, J., Chervin, R. M., and Jenne, R. L.: Global distribution
865 of total cloud cover and cloud types over land, NCAR Tech. Note NCAR/TN-
866 273+STR, National Center for Atmospheric Research, Boulder, CO, 29 pp. + 200
867 maps, 1986.

868 Wood, R.: Stratocumulus clouds, *Mon. Wea. Rev.*, 140, 2373-2423, 2012.

869 Zheng, Y., Zhang, H., Rosenfeld, D., Lee, S. S., Su, T., and Li, Z.: Idealized Large-Eddy
870 Simulations of Stratocumulus Advecting over Cold Water. Part I: Boundary Layer
871 Decoupling, 78, 4089-4102, <https://doi.org/10.1175/JAS-D-21-0108.1>, 2021.

872

873

874

875

876

877

878

879

880

881

882

883

884

885

886

887

888

889

890

891

892

893

894

895

896

897

898

899



900 **FIGURE CAPTIONS**

901

902 Figure 1. A red rectangle marks the simulation domain in the Svalbard area, Norway. The
903 light blue represents the ocean and the green the land area.

904

905 Figure 2. The vertical distributions of the domain-averaged potential temperature and
906 humidity at the first time step.

907

908 Figure 3. Aerosol size distribution at the surface. N represents aerosol number
909 concentration per unit volume of air and D represents aerosol diameter.

910

911 Figure 4. The vertical distributions of the time- and domain-averaged IWC and LWC in
912 the 200_2 and 200_2_noice runs.

913

914 Figure 5. The vertical distributions of the time- and domain-averaged deposition and
915 condensation rates in the 200_2 and 200_2_noice runs.

916

917 Figure 6. The vertical distributions of the time- and domain-averaged IWC and LWC in
918 the 200_2, 200_2_noice and 200_2_fac10 runs.

919

920 Figure 7. The vertical distributions of the time- and domain-averaged (a) IWC and (b) LWC
921 in the 200_2, 2000_20, 200_2_fac10, 200_20, 2000_2, 200_2_fac10_CCN10, and
922 200_2_fac10_INP10 runs.

923

924

925

926

927

928

929

930



Simulations	The number concentration of aerosols acting as CCN at the first time step in the PBL (cm ⁻³)	The number concentration of aerosols acting as INP at the first time step in the PBL (cm ⁻³)	ICNCavg/CDNCavg	Ice processes
200 2	200	2	0.220	Present
2000 20	2000	20	0.201	Present
2000 2	2000	2	0.108	Present
200 20	200	20	0.512	Present
200 2 noice	200	2	0.000	Absent
2000 2 noice	2000	2	0.000	Absent
200 2 fac10	200	0.07	0.022	Present
200 2 fac10 CCN10	2000	0.07	0.012	Present
200 2 fac10 INP10	200	0.7	0.041	Present

931

932 Table 1. Summary of simulations

933

934

935

936

937

938

939

940

941

942

943

944

945

946

947

948

949



Simulations	IWC (10^{-3} g m^{-3})	LWC (10^{-3} g m^{-3})	IWP (g m^{-2})	LWP (g m^{-2})	IWC/LWC	IWP/LWP	Condensation rate		Deposition rate		Cloud-base sedimentation ($10^{-3} \text{ g m}^{-2} \text{ s}^{-1}$)		Entrainment (cm s^{-1})
							Over grid points (10^{-2} g m^{-3} s^{-1})	Over cloudy columns (g m^{-2} s^{-1})	Over grid points (10^{-2} g m^{-3} s^{-1})	Over cloudy columns (g m^{-2} s^{-1})	Ice- crystal	Droplet	
200 2	6.57	0.25	31.94	1.23	26.28	25.96	0.11	1.98	1.30	23.40	1.17	0.17	0.25
2000 20	7.82	0.21	40.91	1.08	37.24	37.91	0.09	1.62	1.57	28.26	0.94	0.06	0.53
2000 2	6.55	0.29	31.85	1.46	22.58	21.81	0.12	2.16	1.28	23.04	1.11	0.08	0.28
200 20	7.80	0.20	40.82	1.01	39.00	40.42	0.09	1.62	1.56	28.08	0.97	0.11	0.51
200 2 noice	0.00	2.06	0.00	10.35	0.00	0.00	0.72	12.48	0.00	0.00	0.00	0.36	0.08
2000 2 noice	0.00	2.25	0.00	11.29	0.00	0.00	0.76	12.80	0.00	0.00	0.00	0.14	0.10
200 2 fac10	0.89	0.85	4.27	4.20	1.05	1.02	0.32	5.76	0.35	6.30	0.19	0.28	0.06
200 2 fac10 CCN10	0.79	0.97	3.82	4.83	0.81	0.79	0.38	6.84	0.31	5.58	0.17	0.19	0.07
200 2 fac10 INP10	0.98	0.78	4.73	3.88	1.25	1.22	0.31	5.58	0.39	7.02	0.14	0.22	0.07

950

951 Table 2. The averaged IWC, LWC, IWP, LWP, condensation and deposition rates over all
 952 of grid points and the simulation period in each of simulations. IWC/LWC (IWP/LWP) is
 953 the averaged IWC (IWP) over the averaged LWC (LWP). Also, as shown are the vertically
 954 integrated condensation and deposition rates over each cloudy column which are averaged
 955 over those columns and the simulation period. The average cloud-base sedimentation rate,
 956 which is for each of ice crystals and droplets, over the cloud base and simulation period,
 957 and the average cloud-top entrainment rate over the cloud top and simulation period are
 958 shown as well.

959

960

961

962

963

964

965

966

967

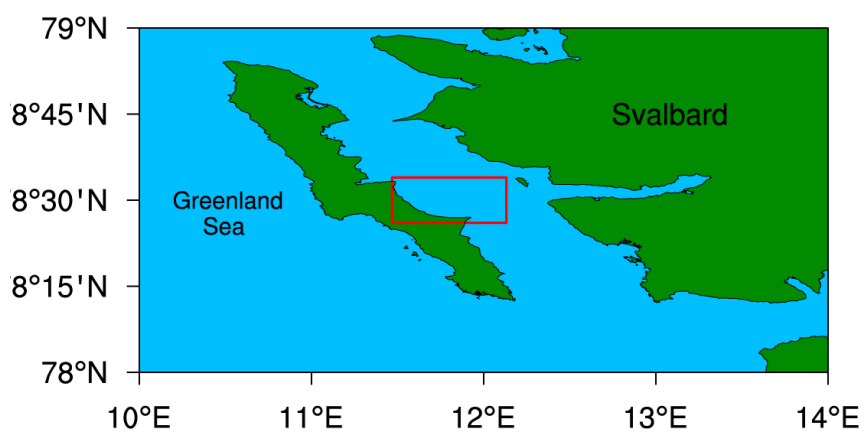
968

969

970

971

972



973

974

Figure 1

975

976

977

978

979

980

981

982

983

984

985

986

987

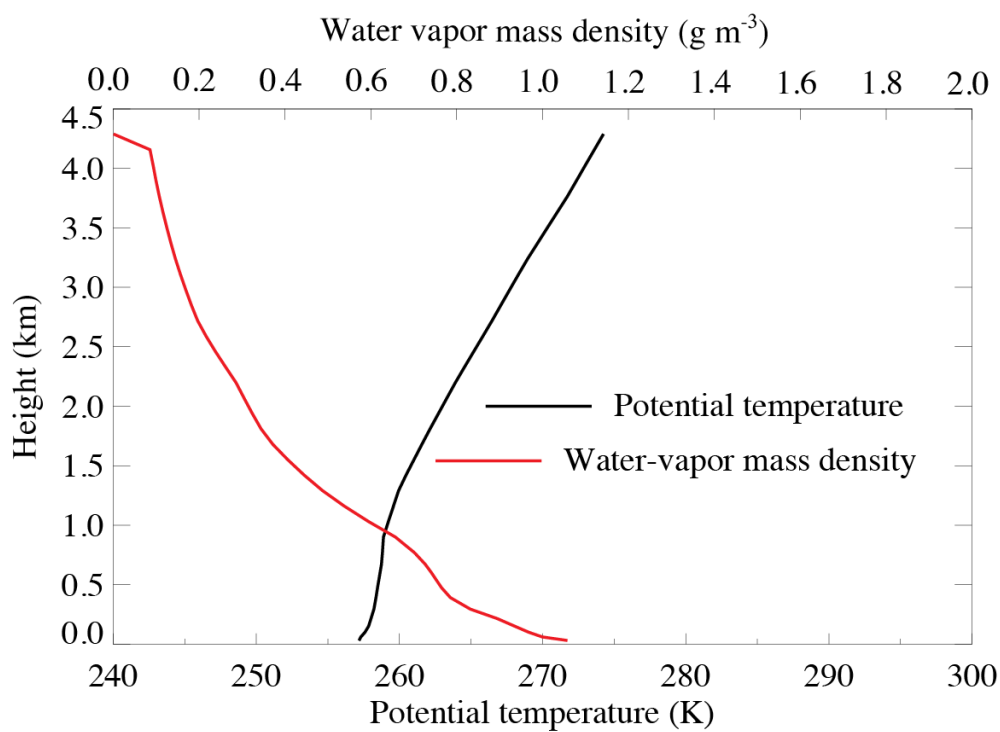
988

989

990

991

992



993

994

Figure 2

995

996

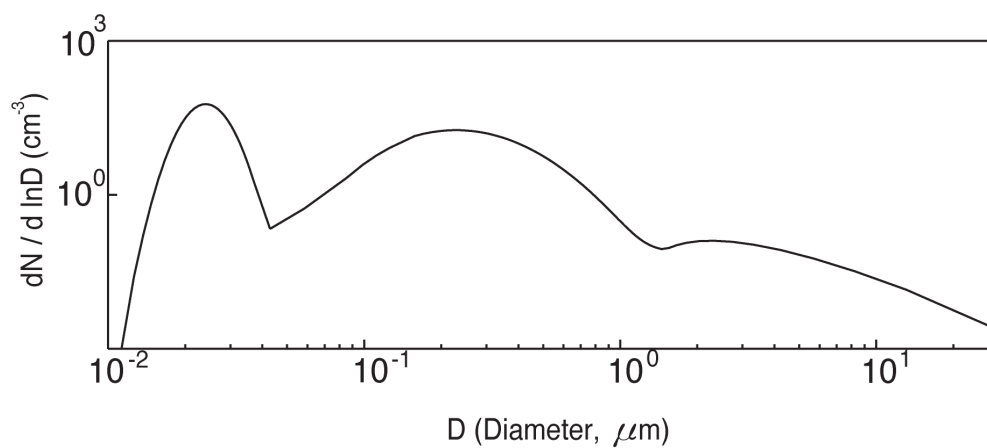
997

998

999

1000

1001



1002

1003

Figure 3

1004

1005

1006

1007

1008

1009

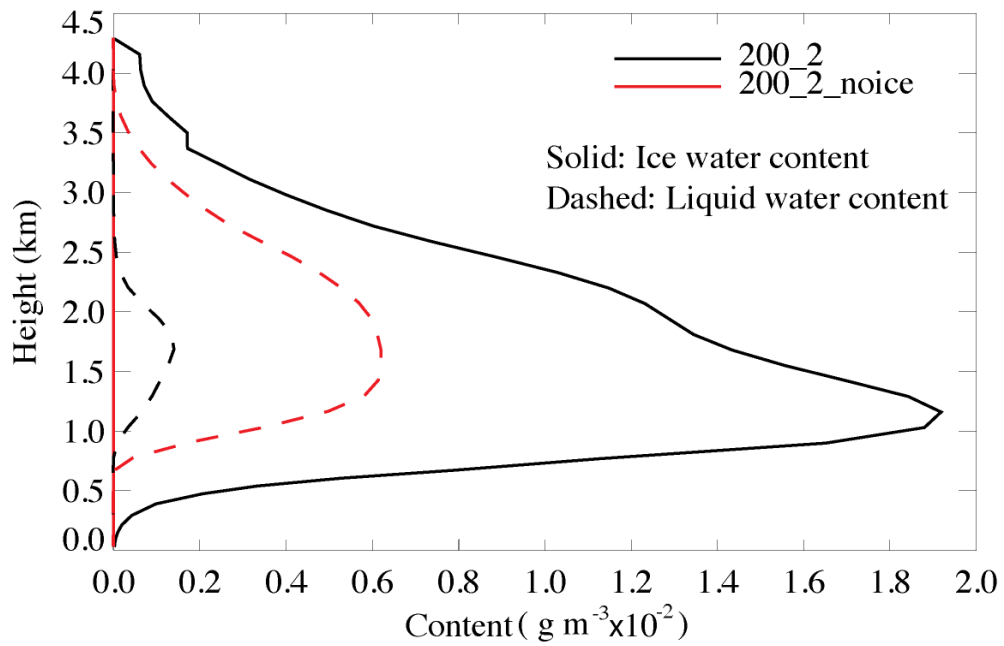
1010

1011

1012

1013

1014



1015

1016

Figure 4

1017

1018

1019

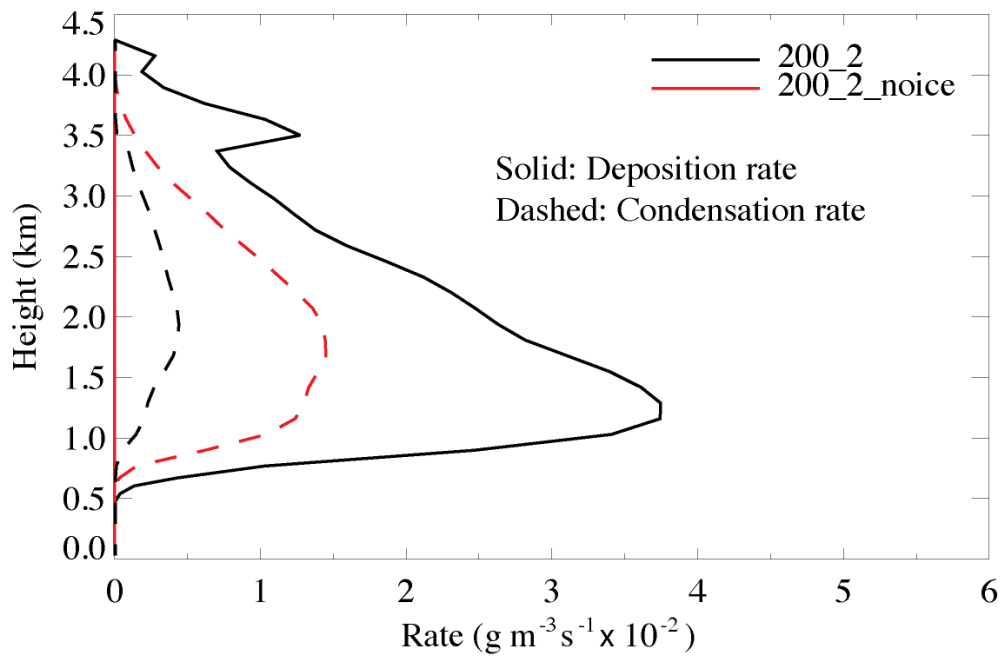
1020

1021

1022

1023

1024



1025

1026

Figure 5

1027

1028

1029

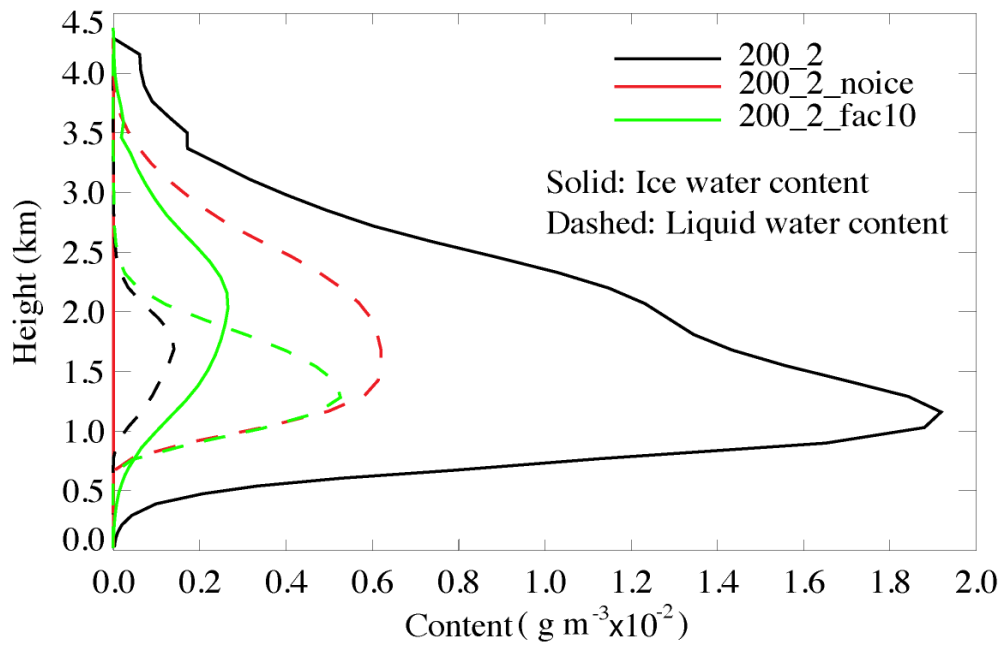
1030

1031

1032

1033

1034



1035

1036

Figure 6

1037

1038

1039

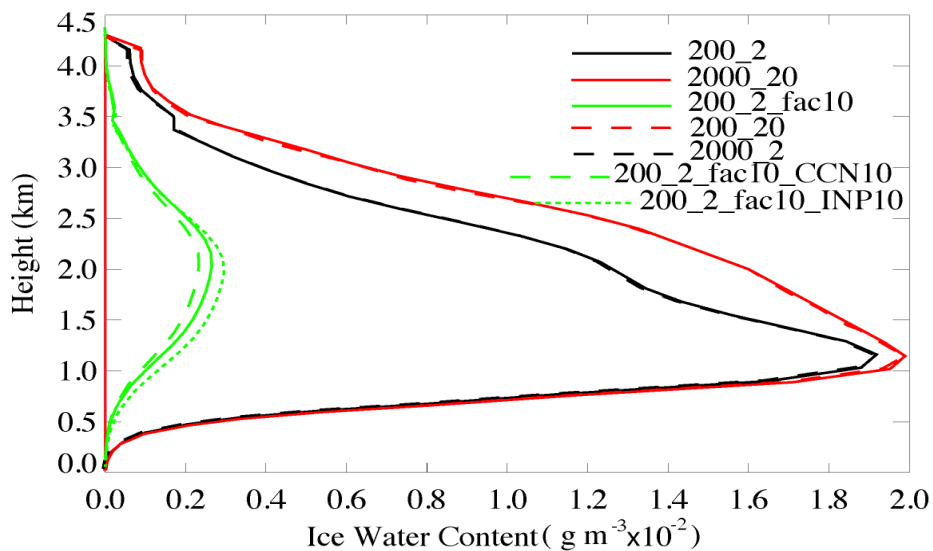
1040

1041

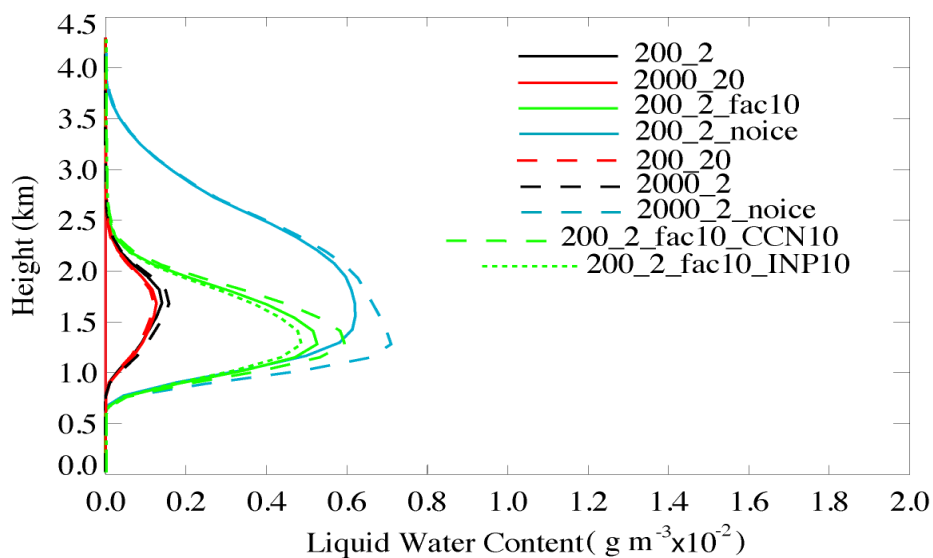
1042

1043

(a)



(b)



1044

1045

Figure 7